THE JOURNAL OF PHYSICAL CHEMISTRY Letters

Letter

Cite This: J. Phys. Chem. Lett. 2019, 10, 4273−4277

pubs.acs.org/JPCL

De- and Recoherence of Charge Migration in Ionized Iodoacetylene

Dongming Jia,[†] Jörn Manz,[†,‡,§,∥] and Yonggang Yang*[,†,∥]

[†]State Key Laboratory of Quantum Optics and Quantum Optics Devices, Institute of Laser Spectroscopy, Shanxi University, Taiyuan 030006, China

[‡]International Center for Chemical Theory, University of Science and Technology of China, Hefei 230026, China

[§]Institut für Chemie und Biochemie, Freie Universität Berlin, 14195 Berlin, Germany

[∥]Collaborative Innovation Center of Extreme Optics, Shanxi University, Taiyuan 030006, China

Supporting Information

ABSTRACT: During charge migration, electrons flow rapidly from one site of a molecule to another, perhaps inducing subsequent processes (e.g., selective breaking of chemical bonds). The first joint experimental and theoretical preparation and measurement of the initial state and subsequent quantum dynamics simulation of charge migration for fixed nuclei was demonstrated recently for oriented, ionized iodoacetylene. Here, we present new quantum dynamics simulations for the same system with moving nuclei. They reveal the decisive role of the nuclei, i.e. they switch charge migration off (decoherence) and on (recoherence). This is a new finding in attosecond-to-femtosecond chemistry and physics which opens new prospects for laser control over electronic dynamics via nuclear motions.

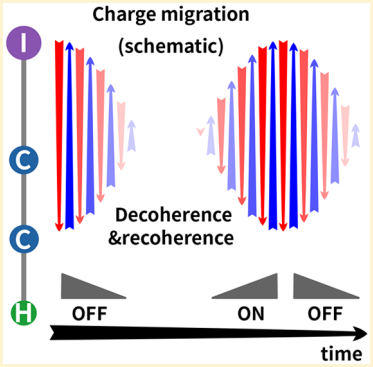

In the process of charge migration (CM), electrons flow rapidly (typically in a few hundred attoseconds) from one site of a molecule to another. CM was discovered experimentally by the group of Schlag and Weinkauf, who pointed immediately to potential applications, e.g. CM might induce selective bond breaking.[1] On the theoretical side, the process was already predicted by H. Eyring et al. in 1944 in their textbook *Quantum Chemistry*,[2] but this was largely forgotten.[3] The experiment[1] aroused the renaissance of the field.[4−10] Comprehensive surveys of the literature are given in refs 11 and 12. A recent milestone is the first joint experimental and theoretical reconstruction of CM by Kraus et al.,[13] specifically in oriented ionized iodoacetylene, $HCCI^+$. Here, we extend their fundamental work by new quantum dynamics simulations not only for the electrons[13] but also for the nuclei; this reveals that the nuclei cause decoherence and recoherence of CM.

The reconstruction of CM by Kraus et al. consists of two steps.[12,13] First, the neutral precursor HCCI in its ground state ($\tilde{X}\ ^1\Sigma^+$, labeled $k = 0$) is ionized within a few femtoseconds (fs) by means of a strong-field laser pulse with linear polarization perpendicular to the molecule to generate the proper experimental initial state $\Psi(t = 0)$ of the oriented cation $HCCI^+$. High harmonic spectra with time resolution of about 100 attoseconds show that $\Psi(t = 0) = C_1\Psi_1 + C_2\Psi_2$ is a superposition of two wave functions Ψ_1 and Ψ_2 which represent the electronic ground state ($\tilde{X}^+\ ^2\Pi$, $k = 1$) and the first excited state ($\tilde{A}^+\ ^2\Pi$, $k = 2$) of $HCCI^+$, respectively.[13] The complex coefficients were thus determined to be $C_1 = 0.90$ and $C_2 = 0.43e^{-0.34i}$. In the second step, quantum dynamics simulations reveal the subsequent CM in the cation $HCCI^+$. A subtle but important detail is that ref 13 considers the nuclear motions in the determination of the initial state but not in the quantum dynamics simulations of the CM. The result is periodic CM between the iodo- and acetylenic moieties of $HCCI^+$. One way takes about 930 attoseconds: this is attosecond electron dynamics. A full cycle back and forth has period $T_{chm} = 1.85$ fs. This period is related to the energy gap $\Delta E = E_2 - E_1$ between the $\tilde{X}^+$ and $\tilde{A}^+$ states at the nuclear geometry of HCCI: $T_{chm}\Delta E = h$, where h denotes Planck's constant. The authors of ref 13 checked carefully that the initial state and its subsequent time evolution were not contaminated by any other states. Accordingly, the experimental populations of the $\tilde{X}^+$ and $\tilde{A}^+$ states of $HCCI^+$ are time-independent, $P_1 = |C_1|^2 = 0.81$ and $P_2 = |C_2|^2 = 0.19$. Here, we adapt the experimental initial state.[13] Preparations of different initial states, e.g. by laser control, may induce different coupled nuclear and electronic dynamics.[11−14]

Here, we extend the previous quantum dynamics simulations[13] to CM in $HCCI^+$ with moving nuclei. The methods profit from well-justified neglect of intermode couplings, adapted from refs 15 and 16; they include a new adaption of the method of Kraus and Wörner[17] for the construction of the initial state prepared by ultrafast ionization of the precursor

Received: June 11, 2019
Accepted: July 9, 2019
Published: July 9, 2019

DOI: 10.1021/acs.jpclett.9b01687
J. Phys. Chem. Lett. 2019, 10, 4273−4277

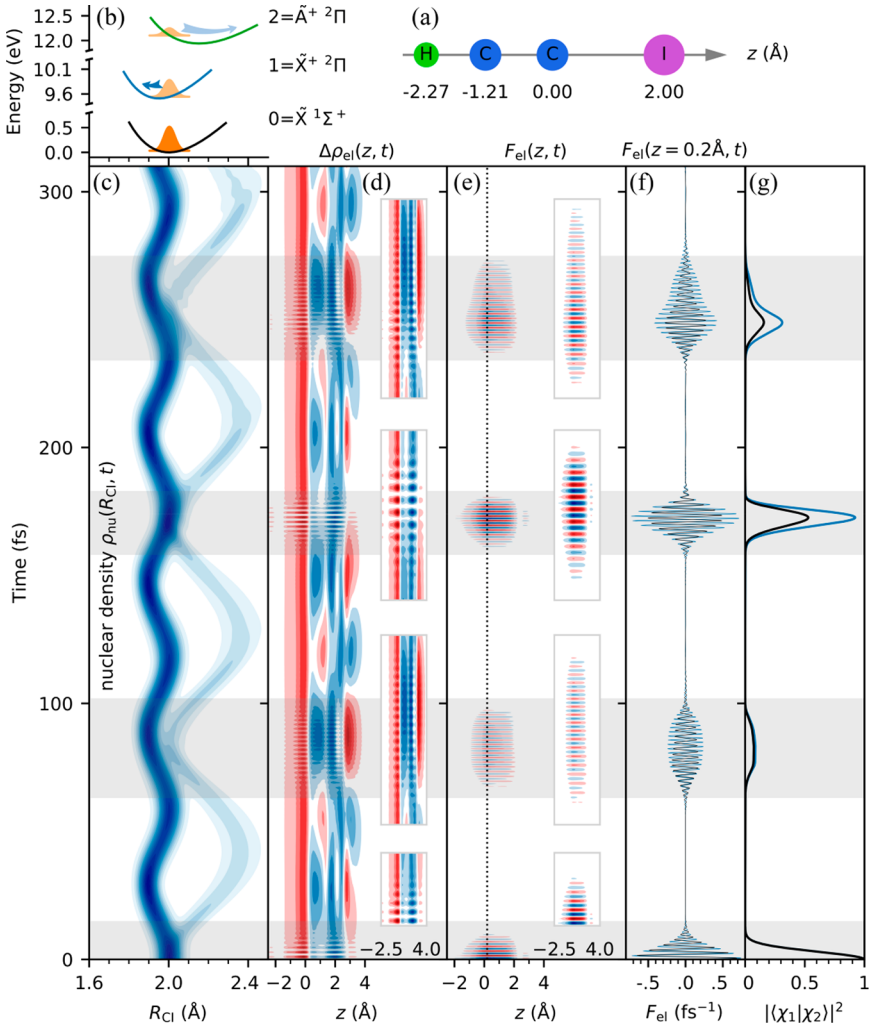

Figure 1. De- and recoherences of charge migration in $HCCI^+$ governed by nuclear dynamics. (a) Schematic of the oriented HCCI molecule. (b) Experimental scenario[13] showing initial nuclear densities embedded in the potential energy curves of HCCI and $HCCI^+$ versus CI bond length R_{CI}. (c) Nuclear density as a function of time, showing large amplitude vibrations of the nuclear wavepackets in electronic states $\tilde{X}^+\ ^2\Pi$ and $\tilde{A}^+\ ^2\Pi$ of $HCCI^+$, which lead to quasiperiodic overlaps. (d) Time evolution of the difference of the electron density along the nuclear axis z at time t compared to the initial density, $\Delta\rho_{el}(z,t) = \rho_{el}(z,t) - \rho_{el}(z,t = 0)$. (e) Time evolution of the electronic flux $F_{el}(z,t)$ along the molecular axis z. (f) Electronic flux $F_{el}(z = 0.2\ Å,t)$ at $z = 0.2$ Å, where it is most prominent (see dashed line in panel e). (g) Absolute square of the overlap of the nuclear wave functions in states $\tilde{X}^+\ ^2\Pi$ and $\tilde{A}^+\ ^2\Pi$. Panels b–g show the results for the one-dimensional (1D) model. Panels f and g compare the 1D (blue lines) and full-dimensional (7D) (black lines) results.

HCCI and new versions of the methods for calculating the electron density and flux along the axis of $HCCI^+$ after ultrafast strong-field ionization of HCCI; for the details, see the Supporting Information. This reveals two key effects of nuclear motions which govern the electronic dynamics: (i) decoherence of CM with decoherence time $\tau_{dec} \approx 6$ fs and (ii) quasiperiodic partial recoherences with period $T_{rec} \approx 170$ fs. The first effect (i) has already been predicted[18] and was observed in several other systems.[15,19−24] The second effect (ii) is a new phenomenon. It is inferable from a simple model[25] but has never been demonstrated previously for any experimental scenario with real molecules or molecular ions. Different effects of ultrafast coupled nuclear and electronic dynamics are, e.g., in refs 26 and 27.

Our results are presented in Figure 1 with seven panels a–g. Details of the methods are provided in several sections of the Supporting Information. The explanations are first presented for the one-dimensional (1D) model that accounts for the most important nuclear degree of freedom (DOF), namely the large amplitude CI stretch (panels b–g). Subsequently, we present analogous results in full (seven) dimensionality (7D, panels f and g). The DOFs will be referred to as the CH, CC, and CI stretches and the pairs of CCH and CCI bends. The complementary three translational and two rotational DOFs are irrelevant.[13] The 1D model is justified by its good agreement with the 7D results (panels f and g). In fact, the decisive role of the CI stretch may be expected from its dominant vibrational progressions in the photoelectron detachment spectrum of HCCI[28] and in the corresponding vibronic distributions of $HCCI^+$ after ultrafast strong-field ionization of HCCI[13] (Supporting Information).

Figure 1(a) shows the geometry of the linear neutral precursor HCCI oriented along the z-direction in the laboratory frame (Supporting Information). Figure 1(b) exhibits the potential energy surfaces $V_k(R_{CI})$ for the neutral precursor HCCI in the electronic ground state $\tilde{X}\ ^1\Sigma^+$ $(k = 0)$ and for the cation $HCCI^+$ in states $\tilde{X}^+\ ^2\Pi(k = 1)$ and $\tilde{A}^+\ ^2\Pi$

DOI: 10.1021/acs.jpclett.9b01687
J. Phys. Chem. Lett. 2019, 10, 4273−4277

(k = 2) (Supporting Information). Also shown in Figure 1(b) are the initial nuclear densities $\rho_{nu,k}(R_{CI},t = 0) = P_k|\chi_k(R_{CI},t = 0)|^2$, where the P_k are the experimental occupations[13] and the χ_k denote the nuclear wave functions in electronic states k = 0, 1, 2 (Supporting Information). The attached curved arrows illustrate the initial directions of the nuclear motions toward CI bond compression (k = 1) and elongation (k = 2). The opposite directions imply rapid initial decay of the overlap $\langle\chi_1(t)|\chi_2(t)\rangle$ of the nuclear wave functions where the Dirac notation $\langle|\rangle$ indicates integration over the nuclear DOF. This conjecture is confirmed quantitatively in Figure 1(g), which shows its absolute square $|\langle\chi_1(t)|\chi_2(t)\rangle|^2$ versus time, with initial decay time $\tau_{decay} \approx 6$ fs.

Figure 1(c) illustrates the time evolution of the nuclear density $\rho_{nu}(R_{CI},t)$, which is the sum of the nuclear densities $\rho_{nu,k}(R_{CI},t)$ for electronic states k = 1, 2 (Supporting Information). The $\rho_{nu,k}(R_{CI},t)$ are essentially periodic. Their periods $T_1 \approx \frac{170}{3}$fs and $T_2 \approx \frac{170}{2}$fs imply alternating weak and strong partial recurrences of $\langle\chi_1(t)|\chi_2(t)\rangle$ at $t \approx$ 85, 170, 255, 340, ..., fs with overall period $T_{1,2} \approx 170$ fs. These recurrences are evident in Figure 1(g). All recurrences have rise times and decay times similar to the initial decay time, $\tau_{rise} \approx \tau_{decay} \approx 6$ fs.

The vibrations of the cation $HCCI^+$ in states k = 1 and 2 cause changes of the electron density $\rho_{el}(x,y,z,t)$ (Supporting Information). For convenience, we center the origin (0,0,0) of the electronic coordinates (x,y,z) at the carbon nucleus that forms the CI bond, and z is the coordinate along the molecular axis (Figure1(a)). We focus on the electronic density $\rho_{el}(z,t)$ along the molecular axis, which is obtained by integrating $\rho_{el}(x,y,z,t)$ over x and y. Figure 1(d) shows the deviation $\Delta\rho_{el}(z,t) = \rho_{el}(z,t) - \rho_{el}(z,t = 0)$ of the electron density at time (t) from the initial density. Obviously, $\Delta\rho_{el}(z,t)$varies on two time scales: A "slow" component, which evolves with the overall period ($T_{1,2} \approx 170$ fs) of the vibrational densities, represents the electrons that move with the nuclei.[29] A "fast" component, which evolves with period $T_{chm} \approx 1.85$ fs, represents charge migration between the iodo and acetylenic moieties of $HCCI^+$. Accordingly, the initial decoherence of CM, with decoherence time $\tau_{dec} \equiv \tau_{decay} \approx 6$ fs, is followed by alternating weak and strong recoherences at $t \approx$ 85, 170, 255 fs, etc., with overall period $T_{rec} \approx T_{1,2} \approx 170$ fs. The recoherences appear with characteristic rise and decay times similar to those for the nuclear recurrences, $\tau_{rec} \approx \tau_{rise} \approx \tau_{decay} \approx 6$ fs. Apparently, the electronic charge migrates if and only if the nuclear densities of $HCCI^+$ in states k = 1 and 2 overlap.

A much more powerful tool for recognizing the de- and recoherences of CM is the electronic flux $F_{el}(z,t)$ along the nuclear axis (Supporting Information),[30] which is plotted in Figure 1(e). It confirms the phenomena revealed by the electronic density in even more pronounced fashion. In brief, the nuclear vibrations (Figure 1(c)) cause quasiperiodic decays and revivals of the overlap of the nuclear wave functions (Figure 1(g)), and these switch off and on the quasiperiodic electronic flux during CM (Figure1(e)). This is confirmed in Figure 1(f), which displays a plot of the electronic flux $F_{el}(z = 0.2$ Å,$t)$ at the position $z = 0.2$ Å (marked by the dashed line in Figure 1(e)), where the electronic flux achieves its maximum value.[30] It has been reported[6,10] that structural changes during charge migration may induce transient localization of electron(s). This can happen during the decoherences in $HCCI^+$ when the flux of migrating electrons decreases, namely part of the electrons are transiently trapped.

The results for the full-dimensional (7D) quantum dynamics simulation of the de- and recoherences of CM in $HCCI^+$ are shown in Figures 1(f) and 1(g). The previous 1D results evidently agree well with these 7D references. Small deviations are discussed in the Supporting Information. This confirms the validity of the 1D model and the analysis of the results.

In conclusion, the present quantum dynamics simulations of the experimental[13] scenario of CM in $HCCI^+$ reveal that adiabatic femtosecond nuclear dynamics governs attosecond electron migration. Accordingly, the quasiperiodic decay and revival of the overlap of the two nuclear wave packets for the two electronic states switches off and on the quasiperiodic CM. The effect cannot be revealed, either by quantum dynamics simulations with frozen nuclei[13] or with Ehrenfest-based classical dynamics simulations of the nuclei.[12,14] The discovery of this principle in the experimental[13] example $HCCI^+$ profits from the well-designed experimental two-state scenario with dominant 1D nuclear dynamics along the large amplitude CI vibration. This suggests HCCI as an ideal system to confirm the phenomena experimentally. Developments of methods for monitoring charge migration with subfemtosecond time resolution are encouraging, see e.g. refs 6, 10, and 31. From the perspective of the CM in the electronic system, it appears that in spite of its decoherence by the nuclei, the nuclei nevertheless serve to keep the memory of the original coherence which is then back-transferred to the CM in the electronic system during the recoherences. This is somewhat analogous to coherent transfer of a superposition state in an electron-spin "processing" qubit to a nuclear-spin "memory" qbit with subsequent coherent back-transfer to the electron spin.[32]

The present discovery of the principle of attosecond CM governed by femtosecond nuclear dynamics opens new prospects for laser control over electronic dynamics via nuclear dynamics. In general, laser pulses can be tailored such that the relevant nuclear wave functions overlap at specified times and molecular conformations. Myriads of scenarios can achieve this goal.[33,34] For the present case of HCCI, one may design, for example, two coherent laser pulses with different carrier frequencies for preparation of $HCCI^+$ in states k = 1 and 2 by resonant photoionization of the oriented precursor. Proper choice of the time delay would then initiate CM in a specific time window even long after the laser pulses. It is gratifying that the experimental technology to generate the required coherent pairs of laser pulses is available.[35,36]

■ ASSOCIATED CONTENT

Supporting Information

The Supporting Information is available free of charge on the ACS Publications website at DOI: 10.1021/acs.jpclett.9b01687.

Details on methods and numerical implementations (PDF)

■ AUTHOR INFORMATION

Corresponding Author

*E-mail: ygyang@sxu.edu.cn

ORCID

Jörn Manz: 0000-0002-9142-8090

Yonggang Yang: 0000-0003-3711-2842

Notes

The authors declare no competing financial interest.

DOI: 10.1021/acs.jpclett.9b01687
J. Phys. Chem. Lett. 2019, 10, 4273−4277

■ ACKNOWLEDGMENTS

We are grateful to Professor Dennis J. Diestler (The University of Nebraska at Lincoln, United States) for careful reading and advice on the manuscript and to Professors Oliver Kühn (Universität Rostock, Rostock) and Herschel Rabitz (Princeton University, Princeton) for valuable guidance to part of the literature. This work was supported in part by the National Key Research and Development Program of China (no. 2017YFA0304203), the program for Changjiang Scholars and Innovative Research Team (no. IRT_17R70), the 111 project (Grant D18001), the Fund for Shanxi "1331 Project" Key Subjects, the talent program of Shanxi, and the National Natural Science Foundation of China (no. 11434007).

■ REFERENCES

(1) Weinkauf, R.; Schanen, P.; Metsala, A.; Schlag, E. W.; Bürgle, M.; Kessler, H. Highly efficient charge transfer in peptide cations in the gas phase: Threshold effects and mechanism. *J. Phys. Chem.* **1996**, *100*, 18567−18585.

(2) Eyring, H.; Walter, J.; Kimball, G. E. *Quantum Chemistry*; Wiley: New York, 1944, Chapter 11.

(3) Diestler, D. J.; Hermann, G.; Manz, J. Charge migration in Eyring, Walter and Kimball's 1944 model of the electronically excited hydrogen-molecule ion. *J. Phys. Chem. A* **2017**, *121*, 5332−5340.

(4) Cederbaum, L. S.; Zobeley, J. Ultrafast charge migration by electron correlation. *Chem. Phys. Lett.* **1999**, *307*, 205−210.

(5) Yudin, G. L.; Chelkowski, S.; Itatani, J.; Bandrauk, A. D.; Corkum, P. B. Attosecond photoionization of coherently coupled electronic states. *Phys. Rev. A: At., Mol., Opt. Phys.* **2005**, *72*, 051401.

(6) Chelkowski, S.; Yudin, G. L.; Bandrauk, A. D. Observing electron motion in molecules. *J. Phys. B: At., Mol. Opt. Phys.* **2006**, *39*, S409−S417.

(7) Remacle, F.; Levine, R. D. An electronic time scale in chemistry. *Proc. Natl. Acad. Sci. U. S. A.* **2006**, *103*, 6793−6798.

(8) Barth, I.; Manz, J. Periodic electron circulation induced by circularly polarized laser pulses: quantum model simulations for Mg Porphyrin. *Angew. Chem., Int. Ed.* **2006**, *45*, 2962−2965.

(9) Kanno, M.; Kono, H.; Fujimura, Y. Control of π-electron rotation in chiral aromatic molecules by nonhelical laser pulses. *Angew. Chem., Int. Ed.* **2006**, *45*, 7995−7998.

(10) Takemoto, N.; Becker, A. Multiple ionization bursts in laser-driven Hydrogen molecular ion. *Phys. Rev. Lett.* **2010**, *105*, 203004.

(11) Jia, D.; Manz, J.; Paulus, B.; Pohl, V.; Tremblay, J. C.; Yang, Y. Quantum control of electronic fluxes during adiabatic attosecond charge migration in degenerate superposition states of benzene. *Chem. Phys.* **2017**, *482*, 146−159.

(12) Wörner, H. J.; Arrell, C. A.; Banerji, N.; Cannizzo, A.; Chergui, M.; Das, A. K.; Hamm, P.; Keller, U.; Kraus, P. M.; Liberatore, E.; Lopez-Tarifa, P.; Lucchini, M.; Meuwly, M.; Milne, C.; Moser, J.-E.; Rothlisberger, U.; Smolentsev, G.; Teuscher, J.; van Bokhoven, J. A.; Wenger, O. Charge migration and charge transfer in molecular systems. *Struct. Dyn.* **2017**, *4*, 061508.

(13) Kraus, P. M.; Mignolet, B.; Baykusheva, D.; Rupenyan, A.; Horný, L.; Penka, E. F.; Grassi, G.; Tolstikhin, O. I.; Schneider, J.; Jensen, F.; Madsen, L. B.; Bandrauk, A. D.; Remacle, F.; Wörner, H. J. Measurement and laser control of attosecond charge migration in ionized iodoacetylene. *Science* **2015**, *350*, 790−795.

(14) Jenkins, A. J.; Spinlove, K. E.; Vacher, M.; Worth, G. A.; Robb, M. A. The Ehrenfest method with fully quantum nuclear motion (Qu-Eh): Application to charge migration in radical cations. *J. Chem. Phys.* **2018**, *149*, 094108.

(15) Arnold, C.; Vendrell, O.; Santra, R. Electronic decoherence following photoionization: Full quantum-dynamical treatment of the influence of nuclear motion. *Phys. Rev. A: At., Mol., Opt. Phys.* **2017**, *95*, 033425.

(16) Yang, Y.; Kühn, O. A concise method for kinetic energy quantisation. *Mol. Phys.* **2008**, *106*, 2445−2457.

(17) Kraus, P. M.; Wörner, H. J. Attosecond nuclear dynamics in the ammonia cation: relation between high-harmonic and photoelectron spectroscopies. *ChemPhysChem* **2013**, *14*, 1445−1450.

(18) Kuleff, A. I.; Cederbaum, L. S. Charge migration in different conformers of glycine: The role of nuclear geometry. *Chem. Phys.* **2007**, *338*, 320−328.

(19) Bandrauk, A. D.; Chelkowski, S.; Corkum, P. B.; Manz, J.; Yudin, G. L. Attosecond photoionization of a coherent superposition of bound and dissociative molecular states: effect of nuclear motion. *J. Phys. B: At., Mol. Opt. Phys.* **2009**, *42*, 134001.

(20) Mineo, H.; Lin, S. H.; Fujimura, Y. Vibrational effects on UV/Vis laser-driven π-electron ring currents in aromatic ring molecules. *Chem. Phys.* **2014**, *442*, 103−110.

(21) Li, Z.; Vendrell, O.; Santra, R. Ultrafast charge transfer of a valence double hole in glycine driven exclusively by nuclear motion. *Phys. Rev. Lett.* **2015**, *115*, 143002.

(22) Vacher, M.; Bearpark, M. J.; Robb, M. A.; Malhado, J. P. Electron dynamics upon ionization of polyatomic molecules: Coupling to quantum nuclear motion and decoherence. *Phys. Rev. Lett.* **2017**, *118*, 083001.

(23) Despré, V.; Golubev, N. V.; Kuleff, A. I. Charge migration in propiolic acid: A full quantum dynamical study. *Phys. Rev. Lett.* **2018**, *121*, 203002.

(24) Lara-Astiaso, M.; Galli, M.; Trabattoni, A.; Palacios, A.; Ayuso, D.; Frassetto, F.; Poletto, L.; De Camillis, S.; Greenwood, J.; Decleva, P.; Tavernelli, I.; Calegari, F.; Nisoli, M.; Martín, F. Attosecond pump-probe spectroscopy of charge dynamics in tryptophane. *J. Phys. Chem. Lett.* **2018**, *9*, 4570−4577.

(25) Cederbaum, L. S. Born−Oppenheimer approximation and beyond for time-dependent electronic processes. *J. Chem. Phys.* **2008**, *128*, 124101.

(26) Sansone, G.; Kelkensberg, F.; Pérez-Torres, J. F.; Morales, F.; Kling, M. F.; Siu, W.; Ghafur, O.; Johnsson, P.; Swoboda, M.; Benedetti, E.; Ferrari, F.; Lépine, F.; Sanz-Vicario, J. L.; Zherebtsov, S.; Znakovskaya, I.; L'Huillier, A.; Ivanov, M. Yu.; Nisoli, M.; Martín, F.; Vrakking, M. J. J. Electron localization following attosecond molecular photoionization. *Nature* **2010**, *465*, 763−766.

(27) Cattaneo, L.; Vos, J.; Bello, R. Y.; Palacios, A.; Heuser, S.; Pedrelli, L.; Lucchini, M.; Cirelli, C.; Martin, F.; Keller, U. Attosecond coupled electron and nuclear dynamics in dissociative ionization of H_2. *Nat. Phys.* **2018**, *14*, 733−738.

(28) Allan, M.; Kloster-Jensen, E.; Maier, J. P. Emission spectra of Cl−C≡C−H $^+$, Br−C≡C−H $^+$ and I−C≡C−H$^+$ radical cations: A $^2\Pi \rightarrow X\ ^2\Pi$ band systems and the decay of the $\tilde{A}\ ^2\Pi$ states. *J. Chem. Soc., Faraday Trans. 2* **1977**, *73*, 1406−1416.

(29) Bredtmann, T.; Diestler, D. J.; Li, S.-D.; Manz, J.; Pérez-Torres, J. F.; Tian, W.-J.; Wu, Y.-B.; Yang, Y.; Zhai, H.-J. Quantum theory of concerted electronic and nuclear fluxes associated with adiabatic intramolecular processes. *Phys. Chem. Chem. Phys.* **2015**, *17*, 29421−29464.

(30) Ding, H.; Jia, D.; Manz, J.; Yang, Y. Reconstruction of the electronic flux during adiabatic attosecond charge migration in $HCCI^+$. *Mol. Phys.* **2017**, *115*, 1813−1825.

(31) Yuan, K.-J.; Shu, C.-C.; Dong, D.; Bandrauk, A. D. Attosecond dynamics of molecular electronic ring currents. *J. Phys. Chem. Lett.* **2017**, *8*, 2229−2235.

(32) Morton, J. J. L.; Tyryshkin, A. M.; Brown, R. M.; Shankar, S.; Lovett, B. W.; Ardavan, A.; Schenkel, T.; Haller, E. E.; Ager, J. W.; Lyon, S. A. Solid-state quantum memory using the ^{31}P nuclear spin. *Nature* **2008**, *455*, 1085−1088.

(33) Shapiro, M.; Brumer, P. *Quantum Control of Molecular Processes*, 2nd ed.; Wiley-VCh: Germany, 2012.

(34) Russell, B.; Rabitz, H. Common foundations of optimal control across the sciences: evidence of a free lunch. *Philos. Trans. R. Soc., A* **2017**, *375*, 20160210.

(35) Goto, H.; Katsuki, H.; Ibrahim, H.; Chiba, H.; Ohmori, K. Strong-laser-induced quantum interference. *Nat. Phys.* **2011**, *7*, 383−385.

DOI: 10.1021/acs.jpclett.9b01687
J. Phys. Chem. Lett. 2019, 10, 4273−4277

(36) Liu, C.; Manz, J.; Ohmori, K.; Sommer, C.; Takei, N.; Tremblay, J. C.; Zhang, Y. Attosecond control of restoration of electronic structure symmetry. *Phys. Rev. Lett.* **2018**, *121*, 173201.

DOI: 10.1021/acs.jpclett.9b01687
J. Phys. Chem. Lett. 2019, 10, 4273−4277